Egyptian Geophysical Society
EGS Journal, Vol. 17, No. 1, 85-100 (2019)

USE OF AZIMUTHAL VERY LOW FREQUENCY–ELECTROMAGNETIC AND MULTI-HEIGHT TERRAIN CONDUCTIVITY METER TECHNIQUES FOR IMAGING NEAR-SURFACE ANCIENT ARCHITECTURAL REMAINS AT TELL HEBUA ARCHAEOLOGICAL SITE, NORTHWEST OF THE EGYPT'S SINAI PENINSULA

K.S.I. FARAG
Geophysics Department, Faculty of Science, Ain Shams University, Abbassia 11566, Cairo, Egypt.

إستخدام تقنيات الكهرومغنطيسية السمتية ذات التردد المنخفض جدا ومقياس التوصيلية الكهربية الأرضية متعدد الإرتفاع لتصوير البقايا المعمارية القديمة القريبة من السطح بموقع 'تل حبوة' الأثرى بشمال غرب شبه جزيرة سيناء المصرية

الخلاصة: تم تنفيذ مسح ميدانى مشترك بإستخدام جسات (سبر رأسية) سطحية لتقنيتى الكهرومغنطيسية السمتية ذات التردد المنخفض جدا ومقياس التوصيلية الكهربية الأرضية متعدد الإرتفاع بمنطقة إختبار مربعة داخل حدود موقع 'تل حبوة' الأثرى بشمال غرب شبه جزيرة سيناء المصرية. تمثل الهدف الرئيسى لهذا المسح فى تسليط الضوء على مدى التطبيق والموثوقية من إستخدام تلك التقنيات السطحية الغير مخترقة –للبنية الأرضية– في مجال دراسى مثل التنقيب الأثرى ومن ثم تصوير تراكيب المقاومة الكهربية الجانبية للبقايا الأثرية المدفونة بالقرب من سطح الأرض. وبالتالى تم تنفيذ ما مجموعه ٨٦١ جسة كهرومغناطيسية سمتية ذات تردد منخفض جدا و ١٧٠١ جسة مقياس التوصيلية الكهربية الأرضية متعدد الإرتفاع موثوق بها فى شهري يناير ٢٠١١ و فبراير ٢٠١٢, على الترتيب. تم تفسير البيانات المقيسة على نطاق واسع ومتسق فى شكل نماذج أرضية ثنائية–البعد سلسة (متدرجة السمك) لكثافة–التيار– الكهرومغناطيسى المكافئة المحولة وللمقاومة الكهربية العكسية, وذلك بدون إستخدام معلومات جيولوجية مسبقة. وبذلك فقد أستخدمت تلك البيانات المفسرة بفعالية وبدون تكلفة عالية لتصوير كلا من جدران الطوب اللبن الطولية –ذات الموصيلية الكهربية المرتفعة– وأحجار الرحى (الطحن) الصغيرة القديمة والمكونة من صخور نارية قاعدية/فوق قاعدية (أو الأجسام الصغيرة والمكونة غالبا من الطوب اللبن عالى الحرق والمدموك) –ذات المقاومة الكهربية المرتفعة– المدفونة جميعا داخل التربة المضيفة –متوسطة المقاومة الكهربية. علما بأن القيم المطلقة لكثافة–التيار–الكهرومغناطيسى المكافئة المحولة رياضيا أو للمقاومة الكهربية المنمذجة عكسيا لم تكن بالضرورة تشخيصية, ولكن التغيرات الرأسية والجانبية لهما قدمت المزيد من المعلومات التشخيصية عن أماكن وأشكال وأحجام وأعماق الدفن للأجسام –ذات التوصيلية/المقاومة الكهربية المرتفعة– وبالتالى إقترحت نماذج جيوكهربية أرضية موثوق بها. هذا وقد أظهرت الدراسة أن مسحا تفصيليا منفذاً بإستخدام جسات الكهرومغناطيسية السمتية ذات التردد المنخفض جدا ومقياس التوصيلية الكهربية الأرضية متعدد الإرتفاع يمكنه أن يساعد فى تصميم برنامج أمثل للحفر الأثرى, ليس فقط لكامل مسطح موقع 'تل حبوة' الأثرى, ولكن أيضا للمدن التأريخية الأخرى المعروفة–ذات المواقع العسكرية المحصنة أو الحامية– بشمال غرب شبه جزيرة سيناء.

ABSTRACT: *A joint azimuthal very low frequency–electromagnetic (VLF–EM) and multi-height electromagnetic–terrain conductivity meter (EM–TCM) sounding survey was conducted at a test square area within the 'Tell Hebua' archaeological site at the northwestern Sinai Peninsula. The main objective of the survey was to highlight the applicability and reliability of utilizing such non-invasive surface techniques in a field like archaeological prospection, and hence to image the lateral electrical resistivity structures of the near-surface buried archaeological remains/objects. Consequently, a total of 861 reliable azimuthal VLF–EM and 1701 multi-height EM–TCM soundings were carried out in January 2011 and February 2012, respectively. The data were interpreted extensively and consistently in terms of two-dimensional (2D) transformed EM equivalent current-density and electrical resistivity smoothed-earth models, without using any geological a-priori information. They could be used effectively and inexpensively to image both the buried linear conductive mudbrick walls and small resistive ancient grinding millstones of basic/ultrabasic igneous rocks (or highly-fired, tightly-compacted mudbrick objects) within the fairly-resistive hosting soil. Absolute transformed EM equivalent current-density or resistivity values were not necessarily diagnostic, but their vertical and lateral variations could provide more diagnostic information about the location, shape, size and depth-of-burial of such existing near-surface conductors/resistors, and hence suggested reliable geo-electric earth models. The study demonstrated that a detailed azimuthal VLF–EM multi-height EM–TCM sounding survey can help design an optimal excavation program, not only for the whole 'Tell Hebua' archaeological site, but also for the other historical fortified garrison towns at the northwestern Sinai Peninsula.*

1. INTRODUCTION

Historically, 'Tell Hebua' (known as Tjaru/Tharu Citadel) was the ancient Egypt's eastern gateway and pharaonic military headquarter in Sinai Peninsula, where the Pelusiac branch of the Nile River once met the Egyptian Mediterranean Sea. This fortified garrison town was initially used by Ahmose–I (New Kingdom era, Dynasty 18) in 16th Century BC to liberate Egypt from Hyksos, and later by Ramses–II (New Kingdom era, Dynasty 19) in 12th Century BC to guard Egypt against Hittites. It was also used to support ancient trading trips to Asia, along the main leading route (known as Way of Horus), and mining expeditions to south Sinai (Sneh and Weissbrod, 1973, Abd El-Maksoud, 1987, Abd El-Maksoud, 1998; Hoffmeier, 2008).

Today, 'Tell Hebua' archaeological site is situated at the Qantara East in Ismailia Governorate (Northwest of the Egypt's Sinai Peninsula), which is located approximately 6.0 km east of Suez Canal and 31.0 km south of the Mediterranean Sea, where the crossed Pelusiac branch of the Nile River is no longer present. It is roughly centered at latitude 30° 55' 52.75" N and longitude 32° 22' 44.65" E (Fig. 1), with an average natural altitude of 2.0 to 4.0 m above the sea level.

Recent excavations carried out by the mission archaeologists of the Egypt's Supreme Council for Antiquities (SCA) since 1980's revealed that the dominant buried architectural style, at the 'Tell Hebua' archaeological site, featured several parallel and cross enclosure and interior mudbrick walls of different thickness, ranging from 0.25 to 4.0 m. These massive walls were made from the raw Nile clayey silt, sundried with seashells and straw to strengthen the mudbrick. They collectively constituted separate or attached rectangular palaces, ramparts, temples, buildings, towers, storerooms, silos, ovens, tombs and open halls of different sizes (Fig. 2a). Throughout, frequent carved hardstone artefacts, column bases, statues and grinding millstones, along with some seals, earthenware and animal remains can be found (Hoffmeier and Abd El-Maksoud, 2003).

Surface electromagnetic induction (EMI) methods involve the measurement of one (or more) magnetic field components which induced within the subsurface by a primary field, produced from a passively-occurred or artificially-generated source, operating at frequencies less than 1 MHz. Most EMI methods have a major advantage, over the other geophysical methods, is that the induction process doesn't require direct (galvanic) contact with the ground. Therefore, the data can be acquired relatively more quickly than other geophysical methods. Such non-invasive techniques are nowadays widely used to image buried archaeological objects without disturbing the ground surface, where such objects are not accurately known or where ground logistics may restrict direct excavation (Scollar, 1962; Tite and Mullins, 1970; Bevan, 1983; Frohlich and Lancaster, 1986; Dalan, 1991; Ogilvy et al., 1991; Bozzo et al., 1992; Lascano et al., 2005; Shendi and Aziz 2010, Timur, 2012).

Consequently, an azimuthal very low frequency–electromagnetic (VLF–EM) survey has been conducted at a test square area within the 'Tell Hebua' archaeological site, covering a surface area of some 40x40 m2, in January 2011. While, a multi-height electromagnetic–terrain conductivity meter (EM–TCM) survey has been conducted at the same test area in February 2012. The main objective was to highlight the applicability, efficiency and reliability of utilizing both the tightly-spaced azimuthal VLF–EM and multi-height EM–TCM surveying techniques (Figure 2b) in a field like archaeological prospection, and hence to image the lateral electrical resistivity structures of the near-surface buried archaeological remains/objects. Accordingly, the vertical and lateral resolution capabilities of such techniques were as necessary as the ability to cover large areas. A total of 861 AVLF–EM and 1701 EM–TCM soundings were carried out along 21 parallel measuring profiles, over the test area, with inter-sounding spacing of about 0.50 to 1.0 m. The topography is very even with no distinct relief, existing relative elevation differences within the test area don't exceed 0.15 m.

2. SOIL AND GROUNDWATER CONDITIONS

The surficial topsoil at the 'Tell Hebua' archaeological site is composed mainly of wind-blown (aeolian transported) very fine-grained silty sand (loess) and underlained essentially by muddy sabkha subsoil of about 0.50 to 1.0 m thick. This is followed by relatively thick salt-affected and smectite-rich Nile Delta (alluvial) clayey sandy silt/silty sand, containing some/traces of shell fragments, clastic ash and broken sherds (Stanley et al., 1998; El-Kashouty et al., 2012). Geomorphologically, they were developed in vast low-lying, poorly-drained coastal flat plains and shallow depressions, belonging to the Holocene to Late Pleistocene age (Fig. 1). Moving southeastward, the highlands surrounding the Tell Heboua archaeological site witness several sand dune and sheet accumulations, derived by the on-shore winds, constitute an outstanding hummocky relief (Belal, 2006).

The soil column at the 'Tell Hebua' archaeological site is always threatened by a free shallow-saline groundwater-table which is encountered between 2.50 to 3.75 m from the existing average natural ground level. It is locally recharged from southwest and its flow is mainly directed towards the north/northeast (El Said, 1994; El-Kashouty et al., 2012).

3. AZIMUTHAL VLF–EM SURVEYING TECHNIQUES

3.1 CONCEPTUAL BACKGROUND

Very low frequency–electromagnetic (VLF–EM) techniques are frequency-domain EMI methods which utilize EM radiation generated by remote, land-based radio-transmitters, distributed all around the world for the purpose of naval military communication with submerged submarines, operating at frequency range from 10 to 30 kHz. These powerful transmitters emit continuously either superimposed frequency-modulated EM wave or occasionally chopped unmodulated Morse code (dots and dashes) (Paal, 1965; Watt, 1967; Paterson and Ronka, 1971; McNeill and Labson, 1991).

The VLF–EM transmitter antenna is effectively a long vertical wire (or rod) mast carrying an alternating current, i.e. vertical electric-dipole. The signal strength is roughly proportional to the amplitude of electric field component parallel to the mast and to the mast length. A radiated (planar) VLF–EM wave consists of coupled vertical electrical and concentric horizontal magnetic fields, perpendicular to each other and to the direction of propagation.

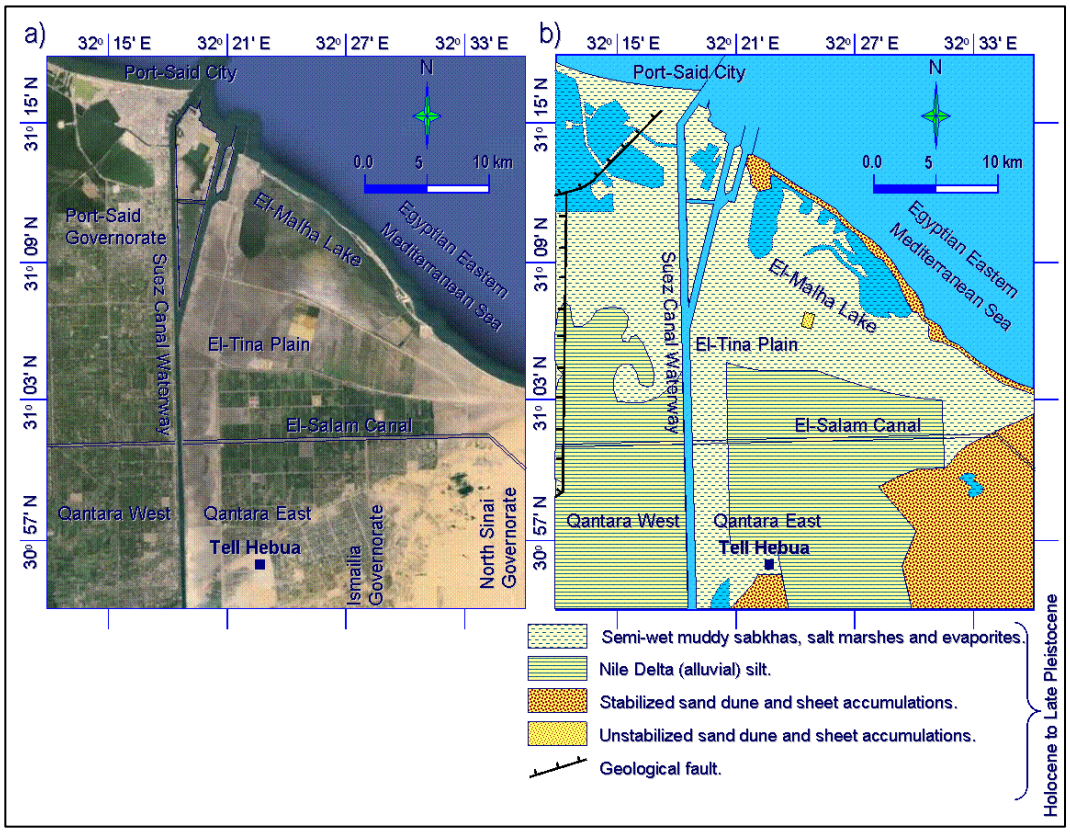

Fig. 1: a) Recent satellite image (courtesy Google Earth™ Mapping Software [Ver. 7.1.2.2041 Beta], Google Inc., USA) and b) surface geologic map (modified after Conco Coral and EGPC, 1987) of the 'Tell Hebua' archaeological site.

Fig. 2: Field photographs showing a) the excavation countryside at 'Tell Hebua' archaeological site and b) the measuring systems Geonics 'EM–31–MK2', b) ABEM 'WADI™ VLF–EM' and c) RadioDetection 'RD–8000'.

It travels efficiently over long distances in the Earth's ionosphere waveguide cavity. Neither the ground nor the ionosphere is a perfect conductor and some VLF–EM energy is lost into space or penetrates the ground. Without this penetration, there would be neither military nor geophysical uses. Induced (eddy) currents in the ground by primary (horizontal) VLF–EM magnetic field produce an opposite secondary (vertical) magnetic field with the same frequency as the primary, but generally with a different amplitude and phase (Fig. 3) depending on the ground resistivity and excitation frequency of the primary field. Any secondary (vertical) magnetic field component is by definition anomalous, causing a tilted or elliptically polarized resultant field.

A VLF–EM magnetic field can be sensed by a small, hand-held receiving (induction) vertical coil in which current flow is in direct proportion to the core permeability, number-of-turns and strength of the magnetic field component(s) along its axis. Furthermore, such a receiving coil reduces the self-capacitance and permits resonant tuning to the selected frequency within the VLF–EM band-pass. In VLF–EM work, the profile direction is almost irrelevant, the critical parameter being the relationship between the known (or presumed) strike of the near-surface conductive archaeological object and the azimuth (or bearing) of the radio-transmitter. An object which strikes towards the radio-transmitter is said to be 'well-coupled', as the primary magnetic field is at right angle to it and induced currents can flow freely. Otherwise, the current flow would be restricted, reducing the strength of the secondary magnetic field.

The measuring procedure for a VLF–EM survey is rather simple, carried out as follows: the receiving coil is tuned to a particular frequency of the selected radio-transmitter. The azimuth of the radio-transmitter is obtained by rotating the coil around a vertical axis until the null position (i.e. minimum coupling) is found. The coil is then rotated around a horizontal axis at right angle to that azimuth (i.e. maximum coupling) where both the real or in-phase (tangent of tilt-angle) and imaginary or out-of-phase (ellipticity/quadrature) components of the complex quantity 'secondary-to-primary fields ratio' or 'scalar tipper function' are noted as percentages through an attached microprocessor in most modern commercial measuring systems. The real component responses are usually very sensitive to near-surface conductors (McNeill and Labson, 1991).

At the 'Tell Hebua' archaeological site, a total of 10 remote radio-transmitters, covering almost the entire VLF–EM frequency band with no gaps, could be detected. These transmitters provide strongly-observed radio-signals and show a wide azimuthal distribution. Their expected geographic locations from which they were initially emitted, based on the measuring azimuths were also noted (Table 1). Therefore, reliable parametric soundings, wherein measurements are made at multiple operating frequencies using a fixed inter-sounding spacing, could then be conducted along the survey profiles, at right-angle to each of those azimuths (Spies and Frischknecht, 1991).

The present field measurements were carried out using the WADI^{TM} VLF–EM system (ABEM Instruments AB, Sweden) (Fig. 2b). Measurements accuracy depends not only on the earth model, but also on field strength, remoteness and departure from the true azimuth of the radio-transmitter, and background noise. Identifying the sources-of-error is crucial in the scalar WADI^{TM} VLF–EM system because it has no real-time series. A procedure to get rough error estimates is by repeating the measurements at every sounding a few times, for each operating frequency, to validate the data and rank the signal strengths of radio-transmitters (Table 1).

These error estimates assess the background noise and can be representative throughout the rest of other soundings. Measurements close to the both local sunrise and sunset timing are routinely avoided. Additionally, the ambient EM noise levels have been regularly assessed in the field using the metal detector 'RD–8000 locating system' (RadioDetection Limited, UK) (Fig. 2d).

3.2 DATA TREATMENT AND INTERPRETATION FLOW

3.2.1 DATA VIEWING

Measured VLF–EM data sets (real Re [%] and imaginary Im [%] components) along the whole survey profiles are usually transferred to a PC computer and completely analyzed (viewed, averaged, filtered and transformed) via the easy-to-use calculating–plotting program CalcView-XL-1.0 (Farag, 2005), as well as using the commercially available software RAMAG^{TM}-2.2 (ABEM Instruments AB, 2002). Their averages are customarily plotted versus measuring distances and collectively presented as a single contoured map (scaled plan view) (Fig. 4).

3.2.2 DATA FILTERING

Fraser (1969) designed a discrete one-dimensional linear filter-operator to enhance the horizontal resolution of local VLF–EM anomalies thereby making them easier to recognize. It shifts the phase of observed VLF–EM data by 90o so that crossovers and inflections will be transformed into peaks to yield contourable anomalies presumably above near-surface conductors. Long spatial wavelengths which result from sounding-to-sounding random geologic noise, nearby topographic effect and other biases are greatly attenuated by such a low-pass smoothing (finite difference) filtering and generally do The filtered output is statistically symmetrical and simply consists of the sum of the measured equispaced VLF–EM data at two consecutive soundings (e.g., Re1 and Re2) subtracted from the sum at the next two consecutive soundings (e.g., Re3 and Re4). The first value is then plotted halfway between sounding positions Re2 and Re3, the second value is plotted halfway between sounding positions Re3 and Re4, and the procedure repeated along the whole data profile. The filtering results are customarily plotted versus measuring distances and collectively presented as a single contoured map (Fig. 5).

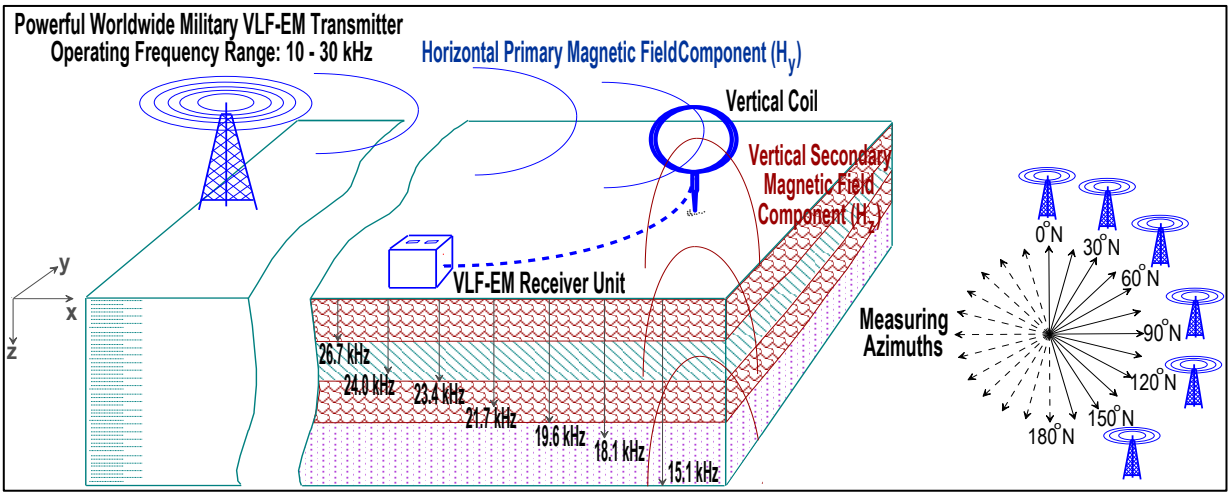

Fig. 3: Field setup of the VLF–EM measuring system, at different azimuths, over an uniform horizontally layered-earth model (redrawn after Farag, 2005).

Table 1: The best-detectable radio-transmitters at the 'Tell Hebua' archaeological site based on their unique azimuths. Their possible geographic locations have been cross-checked for the 180° ambiguity with a maximum departure of ± 10° from the true azimuth of the radio-transmitter. Radio-transmitters information compiled from different sources (ABEM, 1989; McNeill and Labson, 1991; Siebel, 1991; Knödel et al., 1997; Bastani and Pedersen, 2001; Klawitter, 2004; Farag, 2005).

Operating Frequency [kHz]	Measured Averaged Azimuth ±10° [oN]	Call Sign/Code Radiated Power [kW]	Geographic Location [Remarks], Travelled Distance [km]	Received Field Strength [A/m]
15.1	311	HWU–I 200	Le Blanc (Rosnay), France [Navy], 3,189	1.03E-05
16.4	340	JXN 350	Nordland, Norway, 4,193	4.71E-07
18.1	19	RDL 550	Krasnodar Krai, USSR, 1,645	2.14E-06
18.2	115	VTX–III 850	South Vijayanarayanam, India, 5,322	1.06E-06
19.6	312	GBZ 500	Anthorn, UK, 3,691	4.09E-07
20.9	316	FTA 300	Sainte-Assise, France 3,180	2.58E-06
21.7	313	HWU–II 200	Le Blanc (Rosnay), France [Navy], 3,189	1.03E-05
23.4	324	DHO 300	Ramsloh, Rhauderfehn, Germany, 3,170	2.09E-06
24.0	301	NAA 1,000	Maine (Cutler), USA, 8,356	4.71E-07
26.7	330	TBB 350	Bafa, Turkey [Navy], 858	1.47E-05

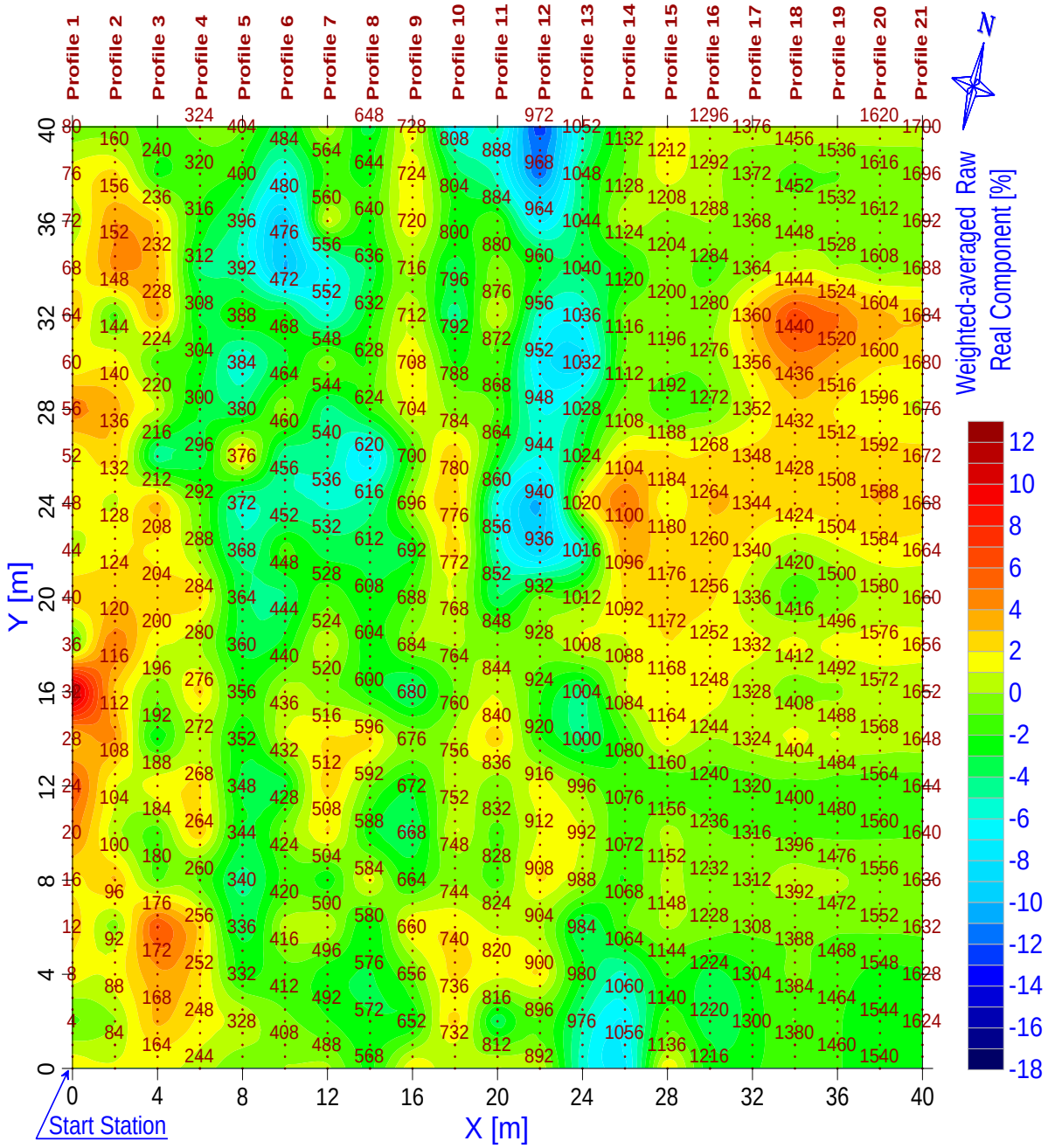

Fig. 4: Weighted-averaged real component contoured maps, using multiple operating frequencies at different measuring azimuths, at the test square area within the 'Tell Hebua' archaeological site. Measuring sounding locations are overlaid. Warm colours (higher real component contours) indicate more conductive near-surface media, while cold colours (lower real component contours) indicate more resistive near-surface ones.

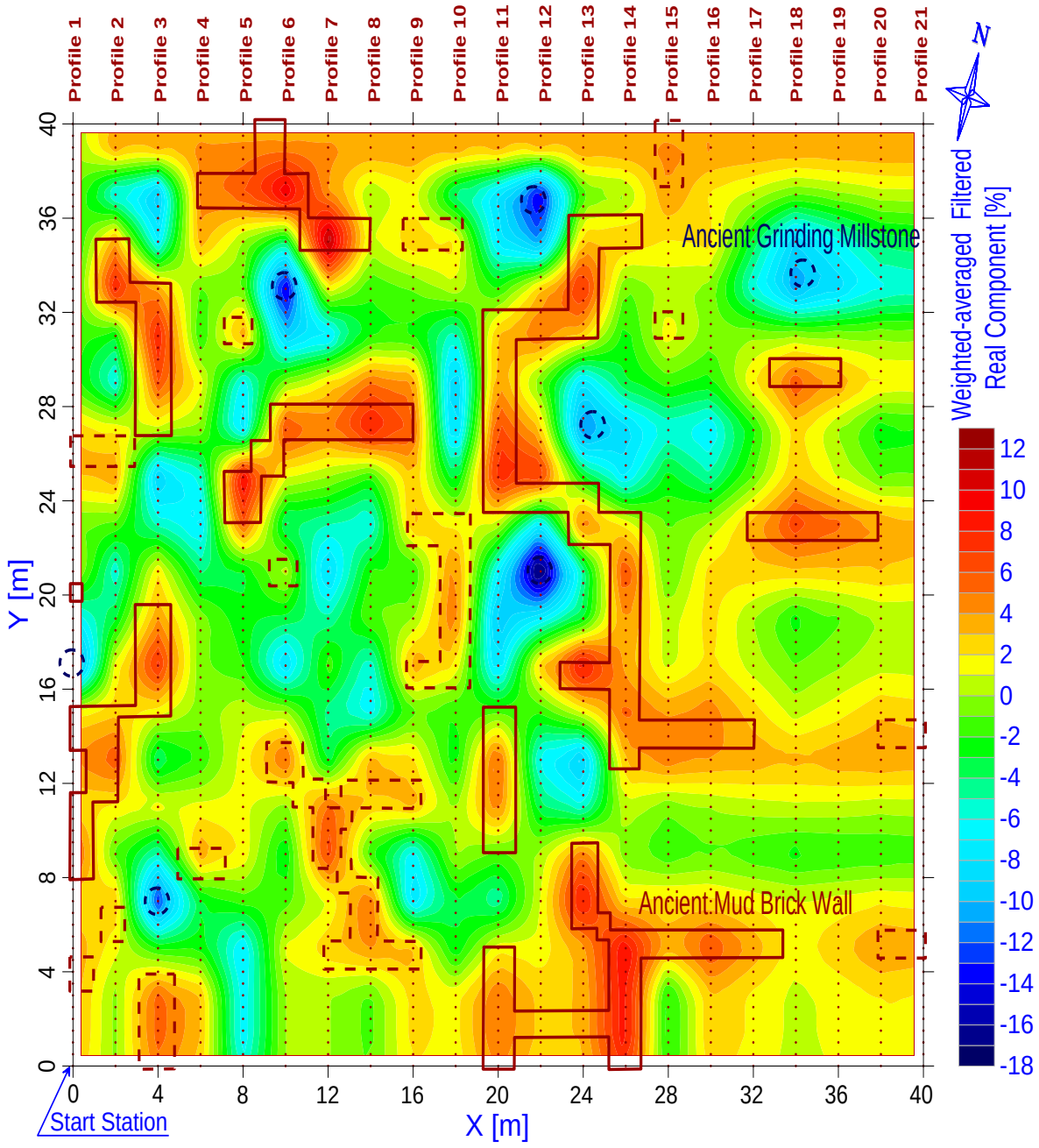

Fig. 5: Weighted-averaged jointly-filtered real component contoured maps, using multiple operating frequencies at different measuring azimuths, at the test square area within the 'Tell Hebua' archaeological site. Warm colours (higher filtered real component contours) indicate more conductive near-surface media, while cold colours (lower higher filtered real component contours) indicate more resistive near-surface ones.

3.2.3 DATA TRANSFORMATION

Karous and Hjelt (1983) designed a more generalized and rigorous form of the widely known Fraser filter-operator, derived directly from the concept of secondary magnetic fields associated with current flow in the earth, to enhance both the horizontal and vertical resolutions of local VLF–EM anomalies. This discrete one-dimensional linear transformation-operator is usually expressed in terms of EM equivalent current-densities at consequent specified depths which consist of both currents induced within the near-surface conductors themselves (i.e., inductive effects) and currents concentrated into the conductors from the less-conducting surrounding (i.e., current gathering). Therefore, the contoured equivalent current-density maxima are always occurred inside the conductors and they do seem to provide reliable depth estimates for such conductors.

The transformed output is statistically symmetrical and simply consists of the sum of the measured equispaced VLF–EM data at three consecutive soundings, multiplied by certain matching coefficients of different polarities, (e.g., –0.102Re1, 0.059Re2 and –0.561Re3) subtracted from the sum at the next three consecutive soundings, multiplied by the same matching coefficients in reverse direction, (e.g., –0.561Re5, 0.059Re6 and –0.102Re7). The obtained value is spatially located below the center sounding Re4 at the depth (level) $\Delta z1$, which is equal to the first data interval (inter-sounding spacing), and normalized by the corresponding $\Delta z1/2\pi$. The computation continues along the whole data profile to obtain the transformed equivalent current densities at such a depth. The procedure is then repeated along the whole data profile using a second (wider) data interval to obtain another current densities for a progressively deeper depth (level) $\Delta z2$, and so on.

The number of depths (levels) is determined by the number of VLF–EM data points along the whole profile. As the operator length is increased each time, weak (suppressed) responses from increasing depths are selectively enhanced as deeper conductors will exhibit long spatial wavelengths (Pirttijärvi, 2004). The transformed equivalent current-densities are customarily plotted as a two-dimensional (2D) contoured pseudo-depth section (scaled cross-section) in a dipole–dipole fashion (Figs. 6 thru 8). Although the VLF–EM techniques are skin-depth limited, where the main controllers are both the operating frequency and bulk ground resistivity, it is worth knowing that the maximum depth-of-investigation for the present transformation is highly controlled by both the survey profile length and inter-sounding spacing.

Both Fraser four-point filtering and Karous–Hjelt six-point transformation have found widespread popularity with field electromagnetists as they introduce simple, readily implemented schemes for semi-quantitative interpretation of observed VLF–EM data (Ogilvy and Lee, 1991). Here, they could provide some diagnostic information about the location, shape, size and depth-of-burial of existing near-surface conductors/ resistors, and hence considered as potentially useful tools for target visualization and discrimination.

4. MULTI-HEIGHT EM–TCM SURVEYING TECHNIQUES

4.1 CONCEPTUAL BACKGROUND

Electromagnetic–terrain conductivity meter (EM–TCM) techniques are frequency-domain EMI methods which use two separate induction coils connected by a reference cable (McNeill, 1980); one coil serves as a transmitter to generate the primary magnetic field within the ground, operating at audio-frequencies, and the other acts as a receiver to sense the earth's induced secondary magnetic field, together with the travelled primary field through the air (Fig. 9). They are generally designed in a way that both coils involve shifting and maintain a fixed small separation between them along the survey profile. Where the induction number, i.e., the inter-coil spacing divided by skin-depth, is much less than unity, then the received complex ratio of the secondary to primary magnetic fields is linearly proportional to the subsurface bulk electrical conductivity (McNeill, 1990). Such moving-dual-coil systems measure the out-of-phase (quadrature) component as the apparent (depth-weighted) conductivity of the ground in milliSiemens per meter [mS/m] and/or the in-phase component in parts per thousand [ppt] at each measuring station along the survey profile. The degree to which these measured components differ, form station to station, can reveal diagnostic information about the electrical and magnetic properties, location, shape, size and depth-of-burial of existing near-surface conductors/resistors. Typically, there are two modes of deployment; horizontal coils with vertical magnetic dipole (VMD) and vertical coils with horizontal magnetic dipole (HMD). The reference point for the measurement is usually the mid-coil position. In VMD orientation the depth-of-investigation is approximately one-and-half to twice the inter-coil spacing, whereas in HMD orientation the depth-of-investigation is approximately one half the inter-coil spacing.

The present field measurements were carried out using the hand-held, single frequency 'EM–31–MK2 system' (Geonics Limited, Canada) (Fig. 2c) which can be employed by one operator. The system consists of an instrument box attached to a shoulder harness strap and centered on a hard PVC boom which maintains fixed separation (about 3.66 m) and orientation between the self-contained, multi-turn coplanar transmitter and receiver coils at each boom's end. The instrument is equipped with the field data logging microcomputer 'Archer–2' for recording, real-time displaying and storing the terrain conductivity (ranging from 10 to 1000 mS/m ± 5.0%) and in-phase (ranging from –20 to +20 ppt ± 5.0%) data sets, along with high-resolution global positioning system (GPS) records.

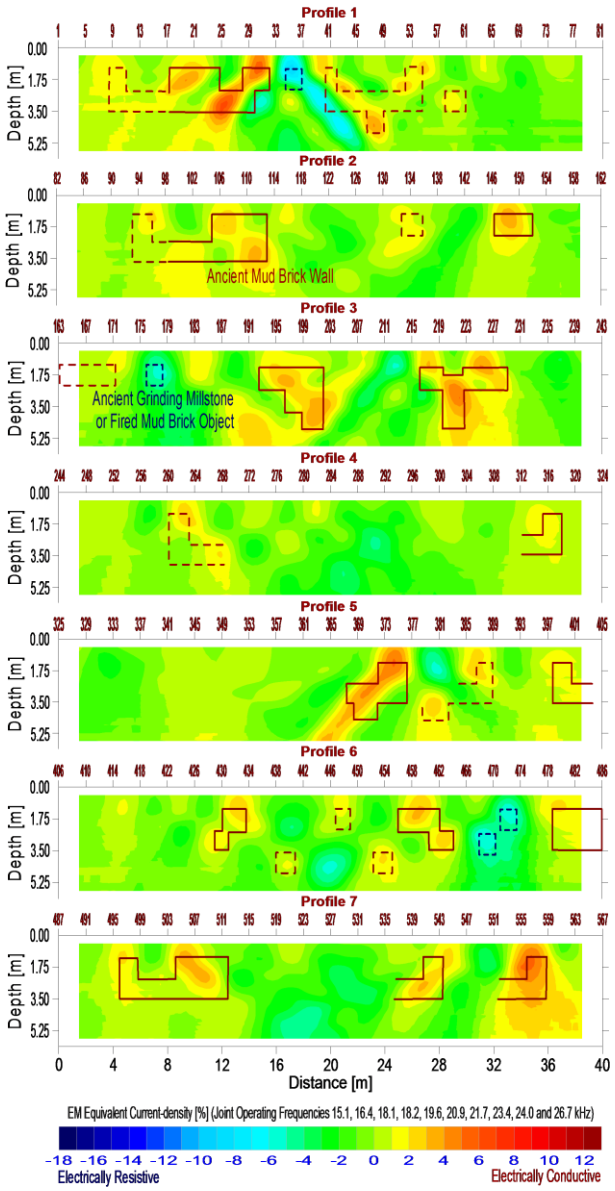

Fig. 6: EM equivalent current-density contoured cross-sections derived from the jointly-transformed real components, using multiple operating frequencies at different measuring azimuths, below the surveying profiles 1 thru 7, at the test square area within the 'Tell Hebua' archaeological site. Warm colours (higher equivalent current-density contours) indicate more conductive near-surface media, while cold colours (lower equivalent current-density contours) indicate more resistive near-surface ones.

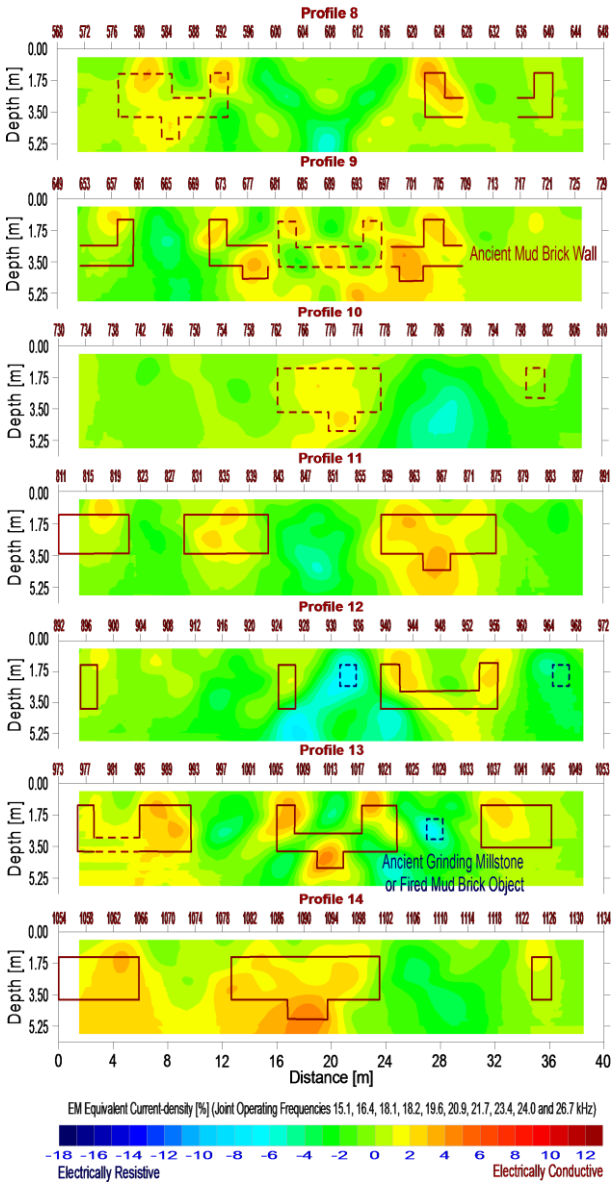

Fig. 7: EM equivalent current-density contoured cross-sections derived from the jointly-transformed real components, using multiple operating frequencies at different measuring azimuths, below the surveying profiles 8 thru 14, at the test square area within the 'Tell Hebua' archaeological site. Warm colours (higher equivalent current-density contours) indicate more conductive near-surface media, while cold colours (lower equivalent current-density contours) indicate more resistive near-surface ones.

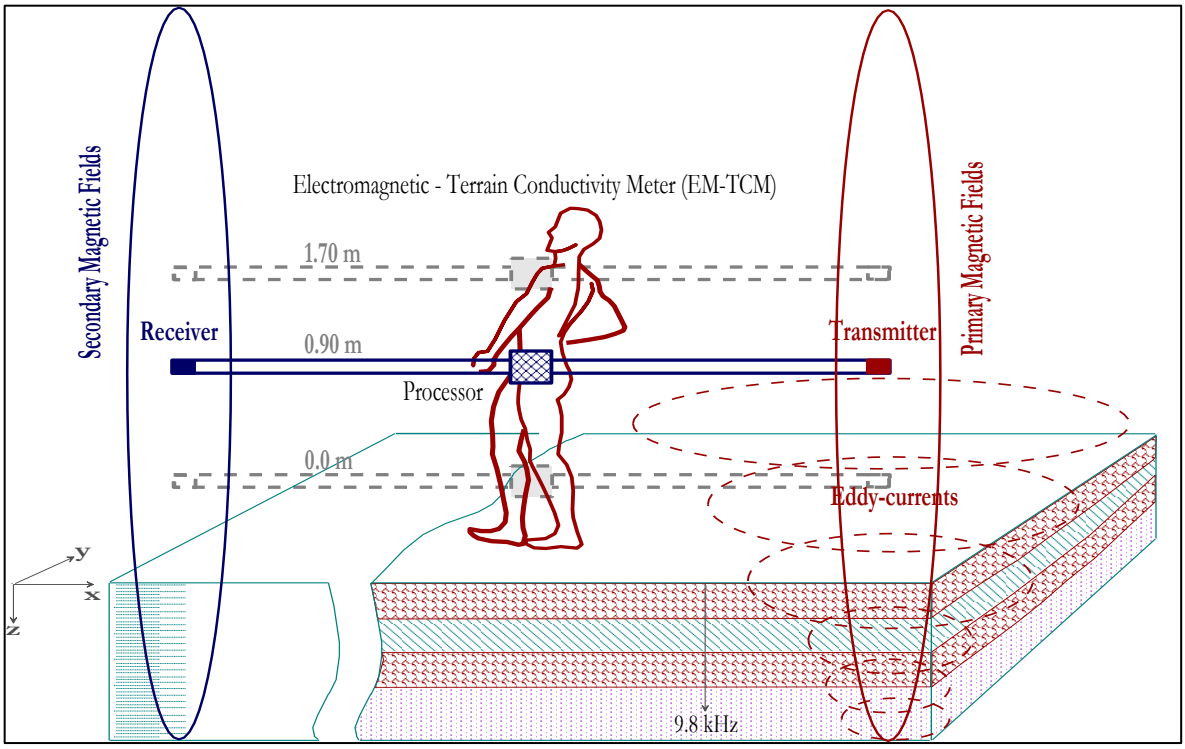

Fig. 9: Field setup of the EM–TCM measuring system, using a varying instrument height above the ground surface at a single operating frequency, over an uniform horizontally layered-earth model (redrawn after Farag and Helal, 2011; Farag, 2015).

Reliable geometric soundings, wherein measurements are made at the single operating frequency (9.8 kHz) using a varying instrument height (approximately ±0.0, 0.90 and 1.70 m above the ground surface), could be conducted along each survey profile (Fig. 9) (McNeill, 1980; Geonics Limited, 2010; Farag and Helal, 2011; Farzamian et al., 2015). Measurements were repeated in forward and backward directions, along each survey profile, and the data were routinely stacked a minimum of 10 times at every sounding for validation. The system was normally operated in its VMD mode, where the central instrument box faces upright and the boom is oriented in the same operator's walking path, along each survey profile. Theoretically, the maximum depth-of-investigation is about 6.0 m deep. The ambient EM noise levels have been regularly assessed in the field using the metal detector 'RD–8000 locating system' (RadioDetection Limited, UK) (Fig. 2d).

4.2 DATA TREATMENT AND INTERPRETATION FLOW

4.2.1 DATA VIEWING

Measured EM–TCM data sets (apparent conductivity σa [mS/m] and in-phase In-Ph [ppt] components) along the whole survey profiles are usually transferred to a PC computer and completely analyzed (viewed, averaged and transformed) via the easy-to-use calculating–plotting program CalcView-XL-1.0 (Farag, 2005). Their averages are customarily plotted versus measuring distances and collectively presented as a single contoured map (scaled plan view) (Figs. 10 and 11).

4.2.2 DATA TRANSFORMATION

For reconnaissance interpretation, EM–TCM data viewing and anomaly mapping/spotting may suffice.

However, the measured interval terrain conductivities at different instrument heights, along each survey profile, in mS/m can be transformed into electrical resistivities in Ohm.m and then plotted against their corresponding normalized resolution depths (levels), i.e., the actual effective skin-depths divided by the inter-coil spacing (Spies, 1989; Farag, 2005; AIDUSH Limited, 2006). They are collectively plotted as a two-dimensional (2D) contoured pseudo-depth section (scaled cross-section) (Figs. 12 thru 14). This simplest form of semi-quantitative interpretation could provide an adequate sampling density, avoiding any spatial aliasing, and hence enhance both the horizontal and vertical resolutions of local EM–TCM anomalies. Therefore, the contoured transformed resistivity minima are always occurred inside the conductors and they do seem to provide reliable depth estimates for such conductors.

5. RESULTS AND DISCUSSION

The resultant azimuthal VLF–EM real component contoured map at the test square area within the 'Tell Hebua' archaeological site (Fig. 4) showed several elongated and cross semi-consecutive positive peaks of ranged intensity and sharpness levels, suggesting the presence of buried conductors at shallow to very shallow

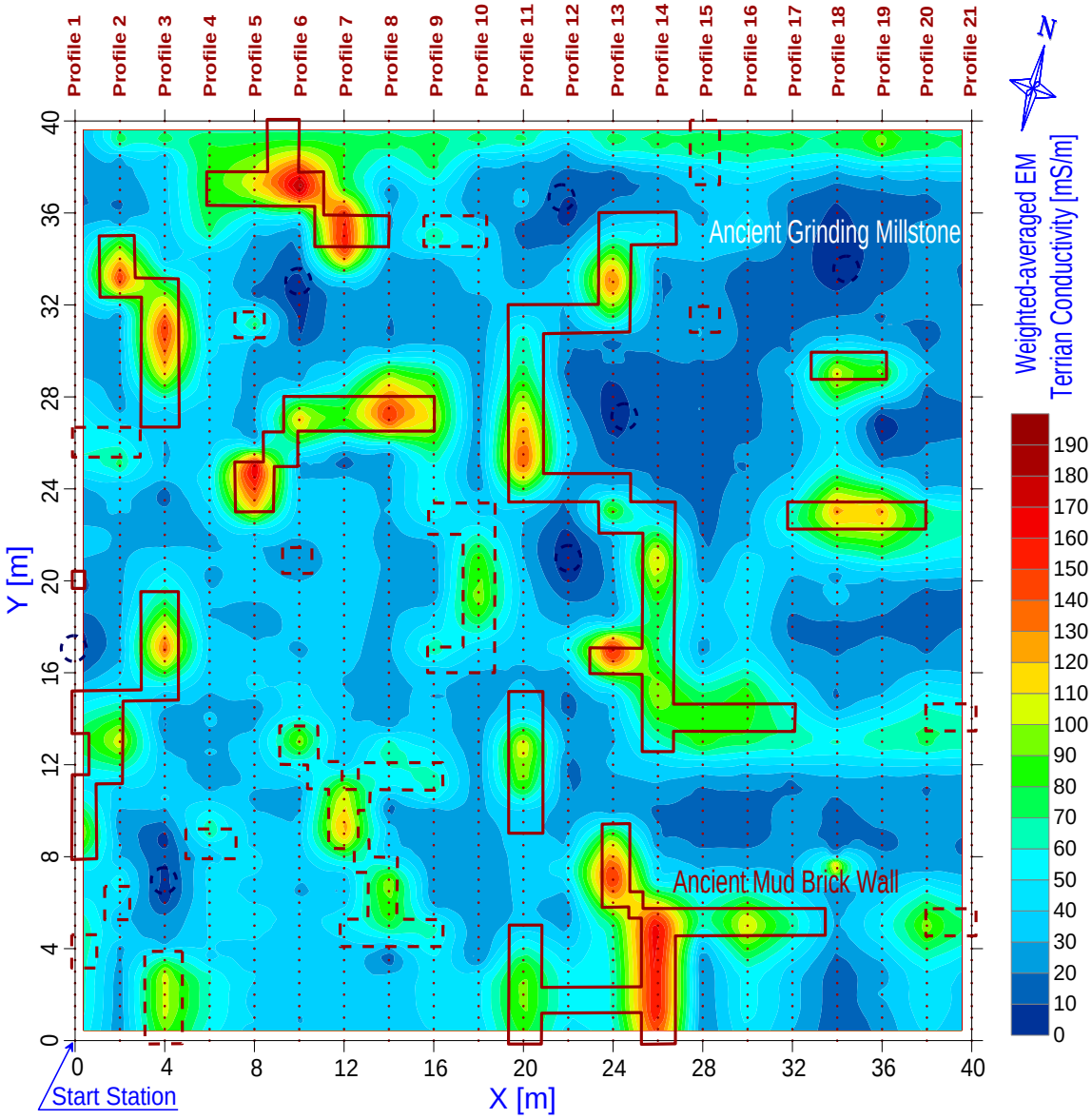

Fig. 10: Weighted-averaged terrain conductivity contoured map, using a varying instrument height, at the test square area within the 'Tell Hebua' archaeological site. Measuring sounding locations are overlaid. Warm colours (higher terrain conductivity contours) indicate more conductive near-surface media, while cold colours (lower terrain conductivity contours) indicate more resistive near-surface ones.

depths. Additionally, they showed small separate negative peaks of limited intensity and sharpness levels, suggesting the presence of localized resistors at very shallow to shallow depths. While, the resultant filtered real component contoured map (Fig. 5) showed more centered, magnified and enhanced consecutive positive and negative peaks over their corresponding linear conductors and small separate resistors, respectively.

The final 2D equivalent current-density cross-sections, derived from the jointly-transformed real components using multiple operating frequencies at different measuring azimuths below the surveying profiles, resulted in a maximum resolution depth-of-investigation of about 6.0 m. The encountered geo-electric sequence (Figs. 6 thru 8) has been shown up with a dominant fairly-resistive hosting soil, constituting mainly of wind-blown silty very fine-grained sand followed by moisturized/saturated clayey/silty sand. This sequence is laterally affected by both near-surface linear anomalies of abrupt high conductivity and localized center anomalies of abrupt high resistivity. The encountered linear anomaly highs may reasonably represent the buried conductive mudbrick walls within the hosting soil. Whereas, the small separate anomaly lows may represent the buried resistive ancient grinding millstones of basic/ultrabasic igneous rocks (or highly-fired, tightly-compacted mudbrick objects) within the hosting soil. Hypothetical schematic drawings, bounding such near-surface objects, have been suggested and laid over both the resultant contoured maps and cross-sections.

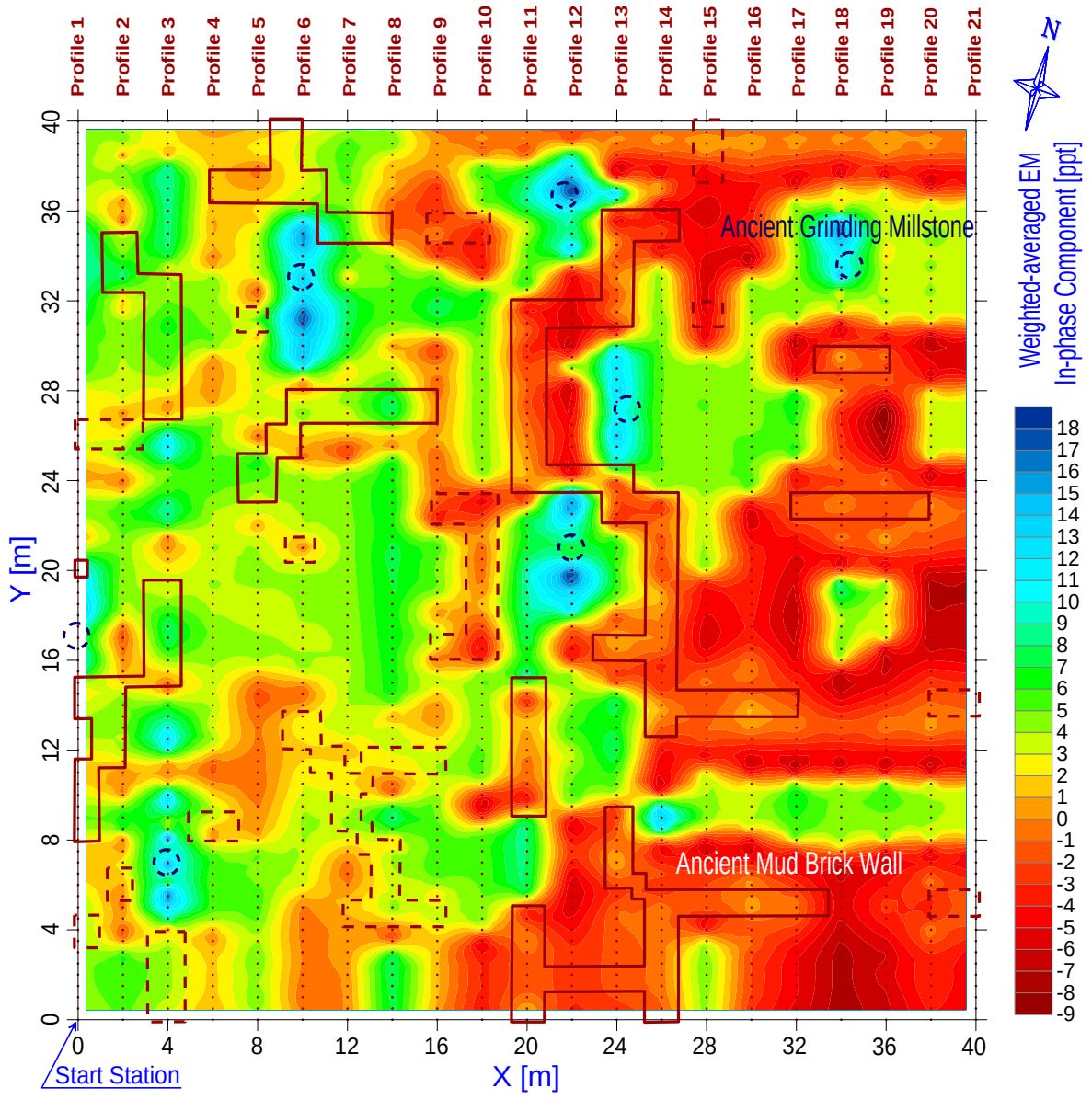

Fig. 11: Weighted-averaged in-phase component contoured map, using a varying instrument height, at the test square area within the 'Tell Hebua' archaeological site. Measuring sounding locations are overlaid. Cold colours (higher in-phase component contours) indicate more ferruginous near-surface media, while warm colours (lower in-phase component contours) indicate less ferruginous near-surface ones.

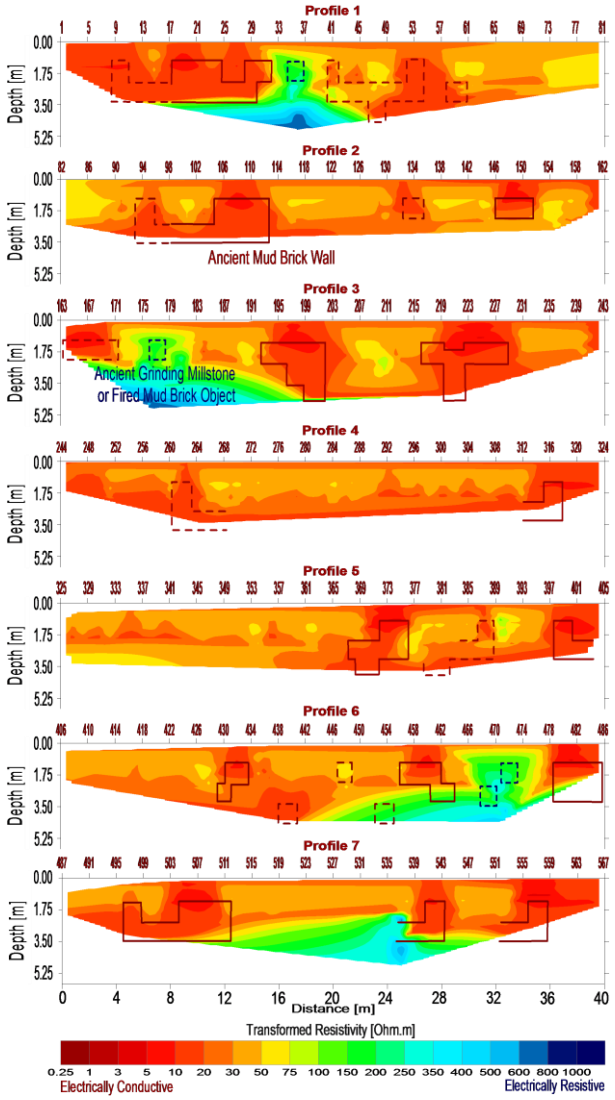

Figure 12: Jointly-transformed electrical resistivity contoured cross-sections derived from the interval EM terrain conductivities, using a varying instrument height, below the surveying profiles 1 thru 7, at the test square area within the 'Tell Hebua' archaeological site. Warm colours (lower transformed resistivity contours) indicate more conductive near-surface media, while cold colours (higher transformed resistivity contours) indicate more resistive near-surface ones.

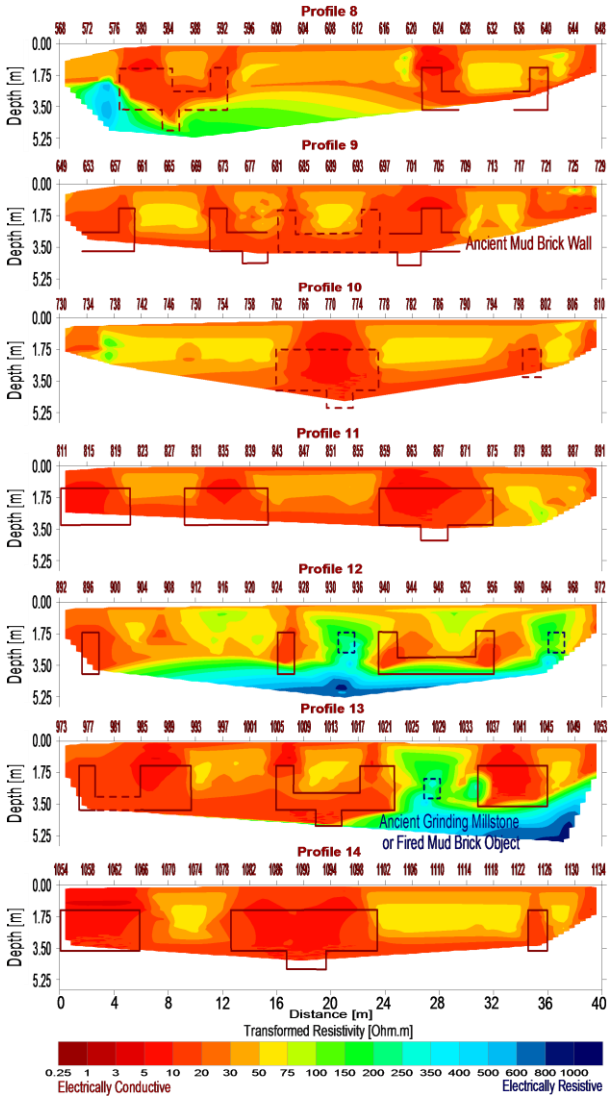

Figure 13: Jointly-transformed electrical resistivity contoured cross-sections derived from the interval EM terrain conductivities, using a varying instrument height, below the surveying profiles 8 thru 14, at the test square area within the 'Tell Hebua' archaeological site. Warm colours (lower transformed resistivity contours) indicate more conductive near-surface media, while cold colours (higher transformed resistivity contours) indicate more resistive near-surface ones.

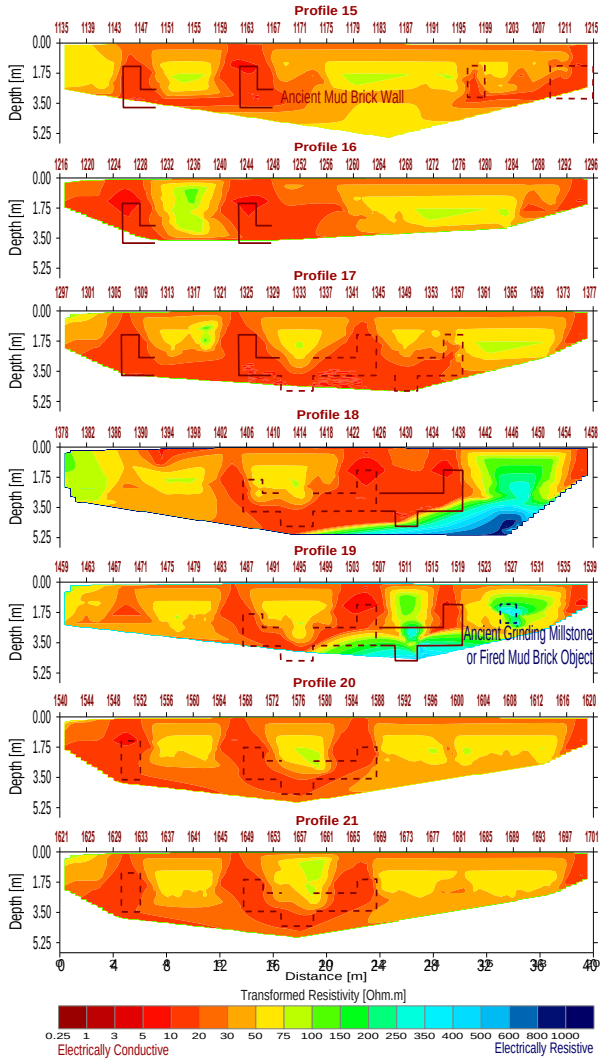

Figure 14: Jointly-transformed electrical resistivity contoured cross-sections derived from the interval EM terrain conductivities, using a varying instrument height, below the surveying profiles 15 thru 21, at the test square area within the 'Tell Hebua' archaeological site. Warm colours (lower transformed resistivity contours) indicate more conductive near-surface media, while cold colours (higher transformed resistivity contours) indicate more resistive near-surface ones.

In agreement, the resultant multi-height EM–TCM conductivity and in-phase component contoured maps confirmed such the characteristic VLF–EM real component lows and highs. The terrain conductivity contoured data (Fig. 10) showed a perceptibly sharp lateral contrast between the buried conductive mudbrick walls and the fairly-resistive hosting soil. For in-phase component contoured data (Fig. 11), there is a broad or undistinguished contrast between the mudbrick walls and the hosting soil, suggesting that the soil materials may contain disseminated inclusions of iron oxides. As the in-phase component positive peaks may describe the anomalous buried ferruginous objects (McNeill, 1983), the encountered positive irregular peaks may verify the presence of ancient grinding millstones of basic/ultrabasic igneous rocks (or highly-fired, tightly-compacted mudbrick objects). Notably, there weren't any near-surface highly-conductive anomalies, indicating metallic signatures (copper, bronze and gold statues or artefacts), as the whole archaeological site was probably pillaged by thieves thru the time history.

The final 2D jointly-transformed electrical resistivity contoured cross-sections, derived from the interval EM terrain conductivities using a varying instrument height below the surveying profiles, resulted in a maximum resolution depth-of-investigation of about 6.0 m. Their earth models were within excellent close proximity to azimuthal VLF–EM equivalent current-density cross-sections (Figs. 12 thru 14). Remarkably, some of the localized center anomalies of abrupt high resistivity, due to the presence of ancient grinding millstones of basic/ultrabasic igneous rocks (or highly-fired, tightly-compacted mudbrick objects), suffered from the EM blanking effect, where their highly-resistive nature usually dominates the measurements and effectively shorts the current flow circuit, leaving very little to penetrate to deeper resistivity structures (Strack, 1992; Farag, 2005).

6. CONCLUSIONS

The present tightly-spaced azimuthal VLF–EM and multi-height EM–TCM field measurements, along with their suggested data treatment and interpretation schemes, demonstrated that their joint results could be used effectively and inexpensively to image both the buried linear conductive mudbrick walls and small resistive ancient grinding millstones of basic/ultrabasic igneous rocks (or highly-fired, tightly-compacted mudbrick objects) within the fairly-resistive hosting soil at the 'Tell Hebua' archaeological site.

Absolute transformed EM equivalent current-density or resistivity values were not necessarily diagnostic, but their vertical and lateral variations could provide more diagnostic information about the location, shape, size and depth-of-burial of such existing near-surface conductors/resistors, and hence suggested reliable geo-electric earth models. Nevertheless, such geo-electric earth models should be used in the context of all available a-priori information. Where necessary, it is deeply recommended that planned hand trial open pits are dug to confirm their location, depth-of-burial and lateral extension.

Finally, this study encourages applying the specially-designed azimuthal VLF–EM and multi-height EM–TCM sounding techniques to reliably image both the vertical and horizontal resistivity structures, resulting from the near-surface buried remains/objects, with a high-resolution. They can even help design an optimal exploration–excavation program, not only for the whole 'Tell Hebua' archaeological site, but also for the other historical fortified garrison towns at the northwestern Sinai Peninsula.

7. ACKNOWLEDGMENT

I am indebted to Dr. Mohamed Abd El-Maksoud, former Head of the Central Department of Lower

Egyptian Antiquities and Director of the 'Tell Hebua' Archaeological Mission (1981–2012), for allowing me to access the site. Special thanks should be go to 'Helal Group for Geotechnical–Geological–Geophysical (3G) Services, Cairo, Egypt' (a private geo-consulting firm operating in Egypt and Arabian countries), for kindly providing WADI™ VLF–EM, Geonics EM–TCM and RadioDetection EM–metal detector measuring systems, during all phases of field measurements.

REFERENCES

Abd El-Maksoud, M., 1987. Une nouvelle forte-resse ur la route D'horus: Tell Heboua 1986 (Nord-Sinaï). Cahier de Recherches de l'Institut de Papyrologie et d'Egyptologie de Lille (CRIPEL), 9, 13–16.

Abd El-Maksoud, M., 1998. Tell Heboua (1981–1991): Enquête archéologique sur la Deuxième Période Intermédiaire et le Nouvel Empire à l'extrémité orientale du Delta. Ministère des Affaires Étrangères, Editions Recherche sur les Civilisations, Paris.

ABEM Instruments AB, 1989. WADI™ VLF–EM International Frequency List. ABEM Printed Matter No. 93062, Bromma.

ABEM Instruments AB, 2002. RAMAG™ Instruction Manual, VLF–EM Survey Planning and Interpretation Software.

Bastani, M. and Pedersen, L.B., 2001. Estimation of magnetotelluric transfer functions from radio transmitters. Geophysics, 66, 1038–1051.

Belal, A.B.A., 2006. Precision Farming in the Small Farmland in the Eastern Nile Delta Egypt using Remote Sensing and GIS. Inaugural-Dissertation zur Erlangung der Doktorwürde der Fakultät für Forst- und Umweltwissenschaften der Albert–Ludwigs–Universität Freiburg im Breisgau, Germany.

Bevan, B.W., 1983. Electromagnetics for mapping buried earth features. Journal of Field Archaeology, 10(1), 47–54.

Bozzo, E., Merlanti, F., Ranieri, G., Sambuelli, L. and Finzi, E., 1992. EM–VLF soundings on the eastern hill of the archaeological site of Selinunte. Boll. Geofis. Teor. Appl., 34(134–135), 169–180.

Conco Coral and EGPC, 1987. Geological Map of Egypt (Scale: 1:500 000, Sheet: NH 36 NW Cairo). In: Klitzsch, E. and List F. K. and Pölmann, G. (Eds.): Egyptian Mapping Project. Geologic Survey of Egypt.

Dalan, R.A., 1991. Defining archaeological features with electromagnetic surveys at the Cahokia Mounds State Historic Site. Geophysics 56(8), 1280–1287.

El-Kashouty, M., El-Sayed, M.H., El-Godamy, Y., Gad M., and Mansour M., 2012. Characterization of the aquifer system in the northern Sinai Peninsula, Egypt. J. Environ. Chem. Ecotoxicol., 4(3), 41–63.

El-Said, M., 1994. Geochemistry of groundwater in the area between El-Qantara and El-Arish, North Sinai. Ph.D. Thesis, Faculty of Science, Ain Shams University, Cairo, Egypt.

Farag, K.S.I. and Helal, A.M.A., 2011. A Multi-frequency VLF–EM Survey for Imaging the Main Metallic Water Pipeline at Al-Alamein City, Northwestern Mediterranean Coast of Egypt. In: 9th Meeting of the Saudi Society for Geosciences (SSG) [1st Arabian Conference of Geosciences], Riyadh, Kingdom of Saudi Arabia.

Farag, K. S. I., 2005. Multi-dimensional Resistivity Models of the Shallow Coal Seams at the Opencast Mine 'Garzweiler I' (Northwest of Cologne) inferred from Radiomagnetotelluric, Transient Electromagnetic and Laboratory Data. Doktorarbeit, Institut für Geophysik und Meteorologie, Universität zu Köln, Cologne, Germany.

Farag, K.S.I., 2015. Imaging Subterraneous Water Regime and Characterizing Soil/Bedrock Conditions at the Ancient Islamic City 'Al-Fustat' (Old Cairo) using Non-invasive Surface Electromagnetic Induction Techniques. 11th International Conference of Geosciences, Saudi Society for Geosciences (SSG), 12–14 May, 2015 at the Campus of King Saud University, Riyadh–Kingdom of Saudi Arabia.

Farzamian, M., Monteiro Santos, F.A. M. and Khalila M.A., 2015. Application of EM38 and ERT methods in estimation of saturated hydraulic conductivity in unsaturated soil. Journal of Applied Geophysics, 112, 175–189.

Fraser, D. C., 1969. Contouring of VLF–EM data. Geophysics, 34(6), 958–967.

Frohlich, B., and Lancaster, W.J., 1986. Electromagnetic surveying in current Middle Eastern archaeology; application and evaluation. Geophysics 51(7), 1414–1425.

Geonics Limited, 2010. EM–31–MK2 (with Archer) Operating Manual. Geonics Limited, 1745

Meyerside Drive, Unit 8, Mississauga, Ontario, Canada, L5T 1C6.

Hoffmeier, J.K. and Abd El-Maksoud, M., 2003. A new military site on the 'Ways of Horus'–'Tell El-Borg' 1999–2001: A preliminary report. J. Egypt. Archaeol., 89, 169–197.

Hoffmeier, J.K., 2008. The archaeology of the Bible. Lion Hudson PLC, Oxford.

Karous, M. and Hjelt S.E., 1983: Linear filtering of VLF dip-angle measurements. Geophysical Prospecting, 31, 782–794.

Klawitter, G., 2004: 100 Jahre Funktechnik in Deutschland: Band1 – Funksendestellen rund um Berlin. Funk Verlag, Berlin.

Knödel. K., Krummel, H. and Lange, G., 1997. Handbuch zur Erkundung des Untergrundes von Deponien und Altlasten: Band 3 – Geophysik. Springer Verlag, Berlin, Heidelberg and New York.

Lascano, E., Martinelli, P. and Osella, A., 2006. EMI data from an archaeological resistive target revisited, Near Surface Geophysics, 4(6), 395–400.

McNeill, J.D. and Labson, V.F., 1991. Geological mapping using VLF radio fields. In: Nabighian, M. N. (Ed.), Electromagnetic Methods in Applied Geophysics, Vol. 2B, Society of Exploration Geophysicists, Tulsa, 521–640.

McNeill, J.D., 1980. Electromagnetic Terrain Conductivity Measurement at Low Induction Numbers. Technical Note TN–6, Geonics Limited, 1745 Meyerside Drive, Unit 8, Mississauga, Ontario, Canada, L5T 1C6.

McNeill, J.D., 1983. Use of EM31 in-phase information. Technical Notes TN–11, Geonics Limited, 1745 Meyerside Drive, Unit 8, Mississauga, Ontario, Canada, L5T 1C6.

McNeill, J.D., 1990. Use of Electromagnetic Methods for Groundwater Studies. In: Ward, S. H. (Ed.), Geotechnical and Environmental Geophysics, Vol. 1: Review and Tutorial, Society of Exploration Geophysicists, Tulsa, 191–218.

Ogilvy, R.D. and Lee, A.C., 1991. Interpretation of VLF–EM in-phase data using current density pseudosections. Geophysical Prospecting, 39, 567–580.

Ogilvy, R.D., Cuadra, A., Jackson, P.D. and Monte, J.L., 1991. Detection of an air-filled drainage gallery by the VLF resistivity method. Geophysical Prospecting, 39(6), 845–859.

Paal, G., 1965. Ore prospecting based on VLF-radio signals. Geoexploration, 3, 139–147.

Paterson, N.R. and Ronka, V., 1971. Five years of surveying with the very low frequency electromagnetic method. Geoexploration, 9, 7–26.

Pirttijärvi, M., 2004. Karous–Hjelt and Fraser Filtering of VLF–EM Measurements: User Manual of the KHFFILT Program Version–1.1a. University of Oulu, Department of Geosciences, Division of Geophysics, Finland.

Scollar, L., 1962. Electromagnetic prospecting methods in archaeology. Archaeometry, 5, 146–153.

Shanghai Aidu Energy Technology Co. (AIDUSH) Limited, 2006. User Manual of ADMT–6 Audio-frequency Magnetotelluric System. AIDUSH, Ltd., 466, Chengjian Road, Minhang District, Shanghai, China.

Shendi, E.H. and Aziz, A.M., 2010. Discovery of an ancient pharaoh's temple on the Horus military road, Northern Sinai, Egypt. Arabian Journal of Geosciences, 3(3), 249–255.

Siebel, W., 1991. Spezial-Frequenzliste 9 kHz−30 MHz. Siebel Verlag, Meckenheim.

Sneh, A. and Weissbrod, T., 1973. Nile delta: the defunct Pelusiac branch identified. Science, 180, 59–61.

Spies, B.R. and Frischknecht, F.C., 1991. Electromagnetic sounding. In: Nabighian, M. N. (Ed.), Electromagnetic Methods in Applied Geophysics, Society of Exploration Geophysicists, Tulsa, Vol. 2A, 285–425.

Spies, B.R., 1989. Depth of investigation in electromagnetic sounding methods. Geophysics, 54, 872–888.

Stanley, D.J., Nir, Y. and Galil, E., 1998. Clay Mineral Distributions to Interpret Nile Cell Provenance and Dispersal: III. Offshore Margin between Nile Delta and Northern Israel. JCR, 14(1), 196–217.

Strack, K.M, 1992. Exploration with Deep Transient Electromagnetics. Elsevier, Amsterdam.

Timur, E., 2012. VLF–R studies in the Agora of Magnesia archaeological site, Aydin, Turkey. J. Geophys. Eng., 9(6), 97–101.

Tite, M. S. and Mullins, C., 1970. Electromagnetic prospecting on archaeological sites using a soil conductivity meter. Archaeometry, 12(1), 97–104.

Watt, A.D., 1967. VLF radio engineering. Pergamon Press, New York.